

Received April 8, 2019, accepted June 4, 2019, date of publication June 13, 2019, date of current version July 1, 2019.

Digital Object Identifier 10.1109/ACCESS.2019.2922044

# Cost Optimization for the Coupled Video Delivery Networks

JING CHEN<sup>1</sup>, DIANJI LU<sup>1</sup>, GUIJUAN ZHANG<sup>1</sup>, JINGPING QIAO<sup>1</sup>,  
PINGSHAN LIU<sup>2</sup>, AND REN HAN<sup>3</sup>

<sup>1</sup>School of Information Science and Engineering, Shandong Normal University, Jinan 250358, China

<sup>2</sup>Business School, Guilin University of Electronic Technology, Guilin 541004, China

<sup>3</sup>School of Optical-Electrical and Computer Engineering, University of Shanghai for Science and Technology, Shanghai 200093, China

Corresponding author: Dianjie Lu (ludianjie@sina.com)

This work was supported in part by the National Natural Science Foundation of China under Grant 61572299, Grant 61876102, Grant 61801278, Grant 61762029, and Grant 61602285, in part by the Shandong Provincial Natural Science Foundation of China under Grant ZR2019MF017, Grant ZR2019BF032, and Grant ZR2017QF008, in part by the Guangxi Natural Science Foundation under Grant 2016GXNSFAA380011, and in part by the Funding for Study Abroad Program by the Government of Shandong Province, Shanghai Science and Technology Innovation Action Plan Project under Grant 17511109100.

**ABSTRACT** Video delivery networks (VDNs) are one of the key enablers for alleviating contradiction between demands increasing for online video and response time of users accessing video content. However, existed works mainly adopt either proactive or reactive delivery scheme, which leads to the problems of backbone traffic overloaded and delays increased. In these works, the impact of performance indicators, such as bandwidth, delay, and personalized demand on delivery cost are not comprehensively taken into account. To overcome these problems, we propose a cost optimization for coupled video delivery model (CO-CVDM), which combines coupled proactive delivery and coupled reactive delivery method to minimize delivery cost in terms of bandwidth consumption, delay performance, personalized demand and construct a multicast delivery tree for the video delivery. The coupled delivery cost minimization problem under constraint conditions is formulated. Since this problem is NP-hard and is prohibitively difficult to solve, we develop a heuristic multicast delivery tree (HMMDT) algorithm to provide more optimized approximate cost. Based on this, we extend CO-CVDM to distribute video in a dynamic scenario. Specifically, with dynamic change of user's requirement for video, the process of video delivery is truncated into a sequence of static graphs and the change of interest attenuation is modeled with human forgetting curve. Finally, the numerical simulations are conducted to validate the advantage of CO-CVDM in terms of optimization delivery cost, and the delivery cost is inversely proportional to the attenuation of user interest.

**INDEX TERMS** Coupled video delivery, cost optimization, bandwidth, delay, personalized demand.

## I. INTRODUCTION

Driven by the digitization of video application and the tremendous popularity of smart device, video alter the way to deliver information. The content of Internet services provided static web pages and Mini Game has been replaced by high-definition video, online short video and so on, as a result of improving technology and emerging applications. Due to social media sharing, online video has given rise to a explosive growth of network traffic [2], [3]. According to prediction by Cisco, video-over-IP traffic will reach

The associate editor coordinating the review of this manuscript and approving it for publication was Francesco Piccialli.

82 percent of all consumer network traffic and online video traffic will be 13 percent of internet video traffic by 2021. Besides, online video traffic will grow fifteen-fold between 2016 and 2021 [4]. For instance, the most popular online video library, YouTube updates more than 1 billion users per month. As reported by a survey [5], the number of network users arrived at 802 million by June 2018 and internet penetration rate was 57.7 percent in China. In additional, the number of internet video users reached 609 million, accounting for 76 percent of the total number of internet users. With the driven video applications and the innovation of application software, more and more services are brought to users. However, data traffic of online video increases

exponentially. Therefore, online video puts higher demands on bandwidth and response time. Dobrian *et al.* [6] pointed out that only 1% of buffering ratio increase can lead to at least three minutes of reduction in the user engagement for a popular 90 minute soccer game. Additionally, the dynamic nature of the network is more significant, and the video content is more diversified because of mobile terminals accessing such as smartphones and tablets. Improving quality of video service and enhancing user experience becomes one major challenge for video applications. Consequently, how to meet the explosive growth of video multimedia demand on limited internet resources, reduce bandwidth consumption, minimize access delay and optimization delivery cost have become a challenging issue in the field of video delivery networks.

Video Delivery Networks (VDNs) deploy edge servers across the network. Then, VDNs redirect access requests of user to edge surrogate servers based on comprehensive information including response time, network load balancing and communication status between servers. Consequently, users obtain video from edge servers which closer to clients. VDNs exhibits strong applicability to delivery video content in reliability and extensibility. However, it also has some limitations. Firstly, most existing works adopt either proactive delivery [7]–[9] or reactive delivery [10], [11] scheme. Objects of video will be replicated into surrogate servers prior to requests in proactive scheme, but the capacity of surrogate servers is limited and it is impossible to replicate all the video objects. In reactive scheme, when users request video objects for surrogate server that has not cached requested objects, origin server deliver video objects to surrogate server. Because of constraint bandwidth of backbone network, the load of servers will too high and the response time prolong greatly in reactive scheme. Secondly, the existing algorithms of video delivery are optimized for performance indicators such as delay, bandwidth and content popularity respectively, resulting cost of delivery increased. Finally, the existed scheme of push-pull does not consider the mobility of users and it dissatisfied personalized requirement of mobile users for online video. It is a hot topic that how to delivery video streaming media dynamically and efficiently while reducing response delay, decreasing bandwidth consumption and minimizing delivery cost in wireless networks.

Motivated by the aforementioned problems, the Cost Optimization for Coupled Video Delivery Model(CO-CVDM) is proposed in this paper. This model not only considers bandwidth consumption, delay performance and personalization demand comprehensively, but also meets the requirement of mobile users for online video in dynamic networks, so as to minimize the delivery cost. Our key contributions are summarized as follows:

- 1) The Coupled Video Delivery Model (CVDM) is proposed, which combines coupled proactive delivery and coupled reactive delivery method. In this model, we consider bandwidth consumption, delay performance together with personalized demand

comprehensively and construct a multicast delivery tree for the video delivery.

- 2) Based on the framework, we study the problem of minimizing coupled delivery cost by formulating the optimal coupled video delivery process. A Heuristic Multicast Delivery Tree (HMDT) algorithm is designed to provide more optimized approximate cost as solving this problem is NP-hard.
- 3) The continuous process for video delivery is truncated into a sequence of static graphs and the dynamic demand model for users is constructed according to the sequence. The interest for video of users will change as time flying. Hence we analyze the interest attenuation for video of user over time and formulate of interest attenuation to track the change of user interest so as to minimize the cost for video delivery.

The rest of the paper is organization as follows. Section 2 is contributed to review of related studies on content delivery and CO-CVDM is introduced in Section 3. Then, we present Dynamic Delivery for Personalized Demand Model in Section 4 respectively. Next, numerical experiments are conducted to evaluate the performance of the proposed algorithm in Section 5. Conclusions and research recommendations are described in Section 6.

## II. RELATED WORK

### A. CONTENT PLACEMENT ALGORITHM

The content placement problem was defined as an optimization problem. Many scholars have studied the problem and proposed different solutions to optimization performance such as the hit rate [12], average distribution rate [13], cost saving [14] and so on. By jointly considering the problem of deployment cost for servers such as servers selection and replica placement, Aram *et al.* [15] designed an optimal scheme to minify cost. Wu *et al.* [16] proposed energy efficient bandwidth aggregation strategy which aggregate energy rate adaption, constrained delay unequal protection and quality packet distribution to leverage energy conservation and minimize end to end delay in wireless network [17]. Aiming to minimize energy consumption, Gong *et al.* [18] explored the transmission from origin server to multiple receivers and construct a minimum multicast tree. Fu *et al.* [19] studied the problem of minimum energy consumption and proposed a framework for optimizing energy transmission in delay constrained wireless networks, where information from the source server distributed to all the  $k$  destinations. In QoS-based surrogate server prioritization techniques [20]–[22], clients are assigned to a surrogate server. In order to meet the demands for video of user, Zeng *et al.* [23] presented a new method of QoS aware greedy heuristic algorithm to maximize the storage capacity and optimize the replica placement in cloud storage systems. Wu *et al.* [24] proposed a novel framework which joint raptor coding and video data deliver to achieve high video quality with minimum bandwidth. The popularity of most videos is well studied on the temporal evolution [25], [26]. Popularity-driven content

caching [27] learns the relationship between the future content and its recent access pattern to optimal cache efficiency. Garetto *et al.* [12] considered popular contents that are constantly added into dynamic analysis system to calculate the hit rate of different cache strategies and analyzed the effect of content popularity on the cache performance, which can be effectively captured into a fixed content-based analysis model. In fact, users evaluate video content in a variety of ways and they are unlikely to be interested in a similar set of video content at the same time. Thus, caching the most popular content is not always optimal [28].

Existing approaches have analyzed performance indicators for cost in term of bandwidth, delay or content popularity respectively, resulting in higher delivery cost. Therefore, we propose a problem of minimizing coupled delivery cost which taken into personalized demand, bandwidth and delay account jointly, and design HMDT algorithm to provide optimized approximate cost.

**B. CONTENT DELIVERY SYSTEM**

The way which user accesses to video content is changing due to video streaming of Internet traffic and expansion of cellular networks. Information delivery plays a critical role in the future network [29], [30]. In order to meet behavior changes of user accessing video, several systems of content delivery are provided to satisfy demand of users for various video streaming media. Tadrous *et al.* [31] constructed a new scheme for proactive resource allocation, which deliver video to surrogate servers in advance based on the predictability of user behavior, to reduce bandwidth required for blocking or interruption probability. In heterogeneous networks scenario, a proactive caching policy [32] are conducted to exploit all communication opportunities for mobile users and small base stations, with the goal of reducing congestion on the backhaul link and minimizing costs, e.g., in terms of energy or bandwidth. The work [33] proposed push-based scheme where the most popular contents are pushed to relieve the burden network and eliminate download time in cellular and converged broadcasting network. Caching strategies which introduced in [34] provided an effective strategy aimed at mitigating massive bandwidth consumption by caching the most popular content closer to the edge servers. Because of constrained storage capacity of surrogate server, proactive delivery policy lead to excessive server load. Carlsson *et al.* [10] designed a pull-based dynamic caching to provide guarantees for unpredictable content request rate and updated routing requests periodically through the solution of optimized model. In pull schema, the response time of user accessing video prolongs greatly. Push or pull toward content delivery provides a new perspective for the distribution mechanism. In [35], Guan and Choi investigated the impact of bandwidth consumption and delay performance jointly on delivery cost in static networks and developed an efficient algorithm toward optimization problem in push-pull system. In the content delivery system [36], the frequency for video content provided affects consumers’ choice between the

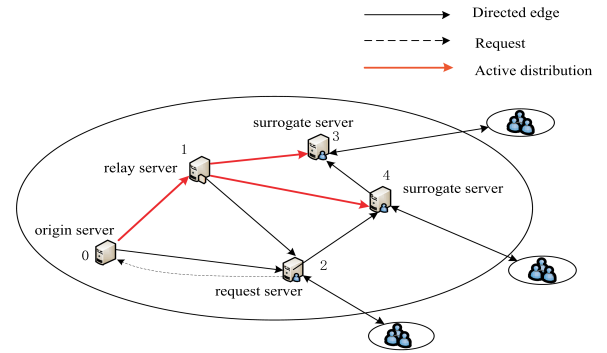


**FIGURE 1. Coupled video delivery model.** 0 represents the origin server, 1 represents the relay server, 2 represents the request server, and 3, 4 represent the surrogate servers. The solid red directed edges corresponds to coupled proactive video delivery process in the figure. The dashed directed edge corresponds to the process of request server sends queries for video objects to origin server when there is not cache user requested video objects. And the solid black directed edges are delivery links.

content pushed to them and pulling content on their own [37]. Guo *et al.* [38] formulated mixed consumption behavior of consumers as push and pull systems, to provide optimal push frequency for content provider.

Extensive research adopt proactive or reactive methods respectively and a few studies for push-pull system explored in static network scenario. They ignored the problem of online video delivery with personalized demands in dynamic networks. The interest of people for video will change over time. Many researchers simulated Ebbinghaus Forgetting Curve to track the change of user interest and applied it to fields such as collaborative filtering and personalized recommendation [39]. Differently, we combine human behavior dynamics and human forgetting feature to learn the changes of user interest and apply it to the field of video delivery. Therefore, we design Dynamic Delivery for Personalized Demand Model in which the process of video delivery is truncated into a sequence of static graphs and analyze the change of user interest attenuation to minimizing delivery cost.

**III. COST OPTIMIZATION FOR COUPLED VIDEO DELIVERY MODEL**

**A. COUPLED VIDEO DELIVERY MODEL**

In our model, we assume that the origin server stores all video streaming media objects. Each surrogate server covers at least one area, and users can request and offload videos from surrogate servers closer to them. To meet the demands of users with limited capacity of surrogate servers, a novel method of Coupled Video Delivery is designed, which combines coupled proactive delivery and reactive delivery method.

In the CVDM (as shown in Fig. 1), the origin server quantify interested degree of users for the video when user send request for a video object to surrogate servers closer to client.  $O_j$  represents the maximum requested number for video objects  $j$  within a period of time and  $O_{ij}$  indicates the number of video streaming media object  $j$  in the surrogate server  $i$ . The origin server evaluates ratio  $O_j/O_{ij}$  to quantify interested degree of users for video objects  $j$  in

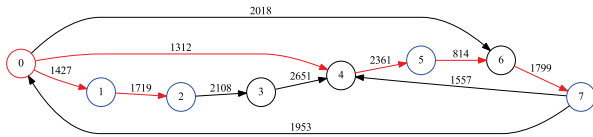


FIGURE 2. Multicast delivery tree model.

the surrogate server  $i$ . In coupled proactive delivery schema, the origin server deliver the video objects to the surrogate servers through the multicast distribution tree according to ratio, then the video objects are replicated into surrogate servers and users forward the video object from surrogate server directly. The process of coupled reactive delivery strategy is as follows: when users send request for video objects to request servers that does not cache those video objects disappointedly, request servers will forward the query to origin server. Then, the origin server sends video objects to the request servers through the multicast distribution tree according to the received video request. Finally, request servers deliver those video objects to the request user. Additionally, we add several relay servers during the process of construction multicast tree to optimize performance of coupled video delivery. Coupled video delivery provide an effective mechanism to reduce the user access delay and relieve bandwidth consumption.

**B. CONSTRUCTING MULTICAST DELIVERY TREE**

The popularity of smart devices for video multimedia induces great demand of bandwidth and lower access delay in mobile network. We take bandwidth, delay and personalized demand into account jointly on coupled video delivery with the goal of minimizing cost. The origin server distributes video objects to surrogate servers by constructing multicast delivery tree in the Coupled Video Delivery model. Several relay servers will be added to enhance performance of video delivery and minimize cost during the multicast delivery tree construction.

In the multicast delivery tree model (see Fig. 2), red node 0 represents the origin server, blue nodes 1, 2, 5, 7 represent surrogate servers or request servers, and black nodes 3, 4, 6 represent the relay surrogate servers. The directed edge between the two nodes corresponds to the communication link among servers, and the number on the directed edge indicates cost of considering bandwidth and delay. The red edge indicates the path we are looking for with the effective cost from origin server to each surrogate or request server.

**C. MINIMIZING COUPLED DELIVERY COST**

Generally, as users request video objects from surrogate server whose area they close to, the delay and bandwidth cost is not effected by allocation of video objects replica. Inspired by the analysis of above for video delivery, we point out that the video delivery networks do not cover the cost of delay and bandwidth among the edge users and the surrogate servers.

In the process of coupled video delivery, the problem of minimizing the coupled cost is designed to satisfy the demand for video objects of user requests and the minimization of bandwidth and delay.

The video streaming multimedia in origin server is divided into  $n$  different video stream objects, and each video stream object is represented by  $s$ . Then the video stream object can be expressed by  $S = \{s_1, s_2, s_3, \dots, s_n\}$ . We denote the storage constraint of each surrogate server  $i$  ( $i = 1, 2, \dots, m$ ) as  $l_i$ .  $\lambda_i$  represents the number of requested video objects that the surrogate server  $i$  forwards. In the process of coupled proactive distribution,  $\theta_{ij}$  indicates the interested degree of users for video object  $j$  in the surrogate server  $i$ , then  $\theta_{ij} = O_j/O_{ij}$ . The variable  $x_{ij}$  indicates whether the video object  $j$  is cached in the surrogate server  $i$ .

$$x_{ij} = \begin{cases} 1, & \text{video object } j \text{ is proactive distributed to surrogate server } i. \\ 0, & \text{video object } j \text{ is reactive distributed to request server } i. \end{cases}$$

The coupled video distribution delay cost can be expressed by:

$$\sum_{i=1}^m \sum_{j=1}^n (1 - x_{ij}) \lambda_i d_{ij} \tag{1}$$

In the formula (1),  $d_{ij}$  represents retrieval delay of the surrogate server  $i$  for the video object  $j$ .

The coupled video distribution bandwidth cost can be formulated as:

$$\sum_{i=1}^m \sum_{j=1}^n (x_{ij} c_j b_{ij} \theta_{ij} + (1 - x_{ij}) \lambda_i c_j b_{ij}) \tag{2}$$

For the formula (2),  $c_j$  indicates the size of the video object  $j$  and  $b_{ij}$  represents the bandwidth of the server  $i$  requesting for video object  $j$ .

When considering cost of bandwidth together with delay, using coefficients  $\alpha$  and  $\beta$  to balance delay and bandwidth to meet a variety of applications and requirements, the subject of minimization cost is as follows:

$$\begin{aligned} & \text{Min}(\alpha \sum_{i=1}^m \sum_{j=1}^n (1 - x_{ij}) \lambda_i d_{ij} \\ & + \beta \sum_{i=1}^m \sum_{j=1}^n (x_{ij} c_j b_{ij} \theta_{ij} + (1 - x_{ij}) \lambda_i c_j b_{ij})) \end{aligned} \tag{3}$$

Similarly,

$$\begin{aligned} & \text{Min} \sum_{i=1}^m \sum_{j=1}^n (\alpha (1 - x_{ij}) \lambda_i d_{ij} \\ & + \beta c_j b_{ij} (x_{ij} \theta_{ij} + \lambda_i (1 - x_{ij}))) \end{aligned} \tag{4}$$

The constraints of formula (4) are as below:

$$\sum_{j=1}^n x_{ij} c_j \leq l_i, \quad i = 1, 2, \dots, m \tag{5}$$

$$b_{ij} \leq b \tag{6}$$

$$0.1 \leq \alpha < 1, \quad 0.1 \leq \beta < 1 \tag{7}$$

$$\alpha + \beta \geq 1 \tag{8}$$

Formula (5) is the storage capacity constraint of server  $i$ . Bandwidth of servers delivery video objects cannot over the maximum bandwidth  $b$  is shown as equation (6). Formula (7) and (8) are constraints for balance factor  $\alpha$  and  $\beta$ .

Next, we review the problem of minimizing coupled delivery cost. Given the size of different video stream objects and the number of requested video objects, is there an allocation strategy such that the total cost in (4) is less than a threshold? Meanwhile, video stream capacity stored in the surrogate server  $i$  is not more than  $l_i$  as in equation (5). The bandwidth satisfies the equation (6), and the relationship of the balanced coefficients satisfy the constraints of the equations (7) and (8).

For the convenience, we only consider a special scenario where single surrogate server with the storage capacity  $l$  is considered. Then, the cost minimization problem is mapped to a set coverage problem and is proven NP-hard. Its complete proof is available in [35]. In the following part, we will give a heuristic algorithm to solve this problem.

#### D. HEURISTIC MULTICAST DELIVERY TREE ALGORITHM

The previous section analysis of the NP-hard problem shows that addressing the problem of minimizing coupled delivery cost lead to tremendous cost. Hence, we propose an effective algorithm, which we called Heuristic Multicast Delivery Tree (HMDT), to obtain better approximate cost. The weight of a node is assigned by the density of the subtree which is rooted at the node and extended the minimal cost path to each terminals [40]. HMDT algorithm continuously adds the minimal weight node and effective cost terminal to this node. Eventually, a cost-effective delivery tree will be constructed where all terminals are included.

We regard the servers in the network as node  $V(v_1, v_2, \dots, v_m)$  and the origin server as root node  $r$ . The terminals represents surrogate/request servers and terminalSet indicates terminal set. Additionally, we generate a directed network graph file, which include root node  $r$ , the number of node, node set  $V$ , terminalSet, the number of directed edges, interested value  $\theta$  and the edges cost between the two nodes. The process of HMDT algorithm is shown in Algorithm 1. Firstly, the parameters are initialized in line 1. Then, for each node  $v$ , we initialize the minimum cost  $rc$  of node  $v$  in line 5. Line 8 is calculates the cost of node  $v$  to each terminals and updates  $rc$  in line 9. In line 11 to 14, the node  $V_{best}$  with the smallest weight are selected according to the cost  $rc$  and the number of node  $n$ . Next, we calculate the cost of the node  $V_{best}$  to each terminal node  $k$  and select terminal node  $k_{min}$  with the lowest cost in line 17 to 19. The node set, delivery path and cost are updated in line 21. Finally, we repeat line 3 to 21 until all terminal nodes are included and find a path with the lowest delivery cost.

According to Algorithm 1, we present the construction process of multicast delivery tree for Fig. 2. To begin with, we identify the node set  $V\{0, 1, 2, 3, 4, 5, 6, 7\}$  and terminalSet $\{1, 2, 5, 7\}$ . Then, we provide the construction steps for multicast delivery tree structure, as shown below.

---

#### Algorithm 1 Heuristic Multicast Distribution Tree

---

**Require:** root node  $r$  in the directed network graph  $G$  file, node set  $V$ ,  $K$  terminals in  $V$ , number of directional edges and cost of each edge

**Ensure:** cost effective delivery path and cost

- 1: Initialize  $T \leftarrow \emptyset, cost(T) \leftarrow 0$ ;
- 2: **while** terminalSet not empty
- 3:    $W \leftarrow \infty, V \leftarrow \emptyset$ ;
- 4:   **for** each node  $v$  in  $G$  **do**
- 5:      $rc \leftarrow$  the lowest cost of node  $v$ ;
- 6:      $n \leftarrow n + 1$ ;
- 7:     **for**(each  $k$  in terminalSet,  $1 \leq k \leq K$ ) and ( $c_j \leq$  available storage of  $v_i$ ) **do**
- 8:       calculate the cost  $rc(v_i, k)$  from  $v_i$  to each terminal  $k$ ;
- 9:        $rc \leftarrow rc + rc(v_i, k)$ ;
- 10:     **end for**
- 11:     **if**( $rc * n < W$ )
- 12:        $W \leftarrow rc * n$ ;
- 13:        $V_{best} \leftarrow v_i$ ;
- 14:     **end if**
- 15:   **end for**
- 16:   **for** each  $k$  in terminalSet,  $1 \leq k \leq K$  **do**
- 17:     calculate the cost of  $V_{best}$  to  $k$ ;
- 18:      $ct \leftarrow$  lowest of  $V_{best}$  to  $k$ ;
- 19:      $k_{min} \leftarrow$  terminal with the lowest cost in terminalSet;
- 20:   **end for**
- 21:    $terminalSet \leftarrow terminalSet - k_{min}, V \leftarrow V - V_{best}, T \leftarrow T \cup \{< V_{best}, W >\}, cost(T) \leftarrow cost(T) + ct$ ;
- 22: **end while**
- 23: **return**  $T$  and  $cost(T)$ ;

---

We initialize the parameters in step 1. Step 2 is initializes the minimum cost  $rc$  of each node  $v_i$ , taking node 0 as an example,  $rc = 0$ . We calculate the cost of node 0 to each terminal node and get  $rc = 12063$  finally in step 3. In step 4, the weight of node 0 is calculated and it satisfy the condition in line 11, then  $W = 48252$  and  $V_{best}$  is node 0. Otherwise none of them not be changed if the condition in line 11 is not satisfied. Additionally, step 5 repeats steps 1 to 4 until all nodes are covered. We find out  $V_{best}$  as node 0 and calculate the cost of node 0 to each terminal, and then we get the lowest cost  $ct = 1427$  and  $k_{min}$  is node 1 in step 6. Next, node set and terminalSet are updated, and we get the path (0,1) and calculate  $cost(T) = 1427$  in step 7. Finally, the delivery path (0,1), (1,2), (4,5), (0,4), (6,7), (5,6) and cost are got repeating steps 1 to 7.

## IV. DYNAMIC DELIVERY FOR COUPLED VIDEO

### A. DYNAMIC DELIVERY FOR PERSONALIZED DEMAND MODEL

Dynamic multicast is required in the coupled multicast video delivery application. The interest for video objects of user has changed over time. Therefore, the surrogate servers and video

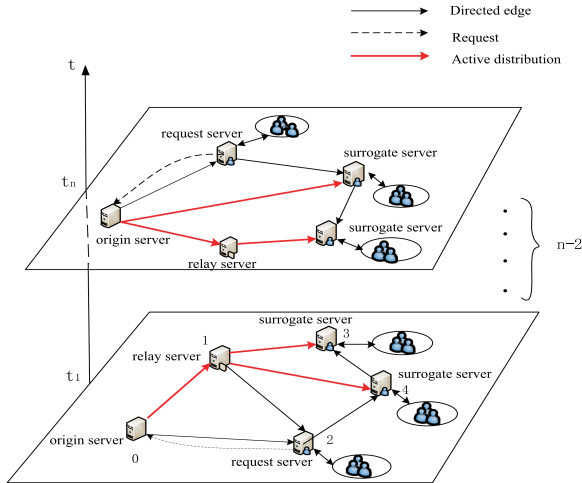


FIGURE 3. Dynamic delivery for personalized demand model.

objects may vary over time in coupled video delivery due to the change of user interest and the request for video randomly.

In order to solve the problem surrogate servers differently and describe the delivery process precisely, the continuous dynamic process is truncated into a series of static graphs  $g = \{g_1, g_2, \dots, g_n\}$  and the Dynamic Delivery for Personalized Demand Model is constructed (see Fig. 3). For instance, the origin server delivers video objects to surrogate servers through the multicast distribution tree according to interest value and requests for video of users in time slot  $t_1$ . In other words, various video objects are delivered to different surrogate servers over time. Furthermore, the method of dynamic coupled video delivery proposed in this paper not only distributes video efficiently, but also satisfies demands of the user to achieve effective cost.

### B. THE FEATURE OF ATTENUATION FOR INTERESTED VIDEO

Because of the complexity of human behavior [41] and the imbalance of human memory forgetting, the interest for video objects of users has changed over time and it takes on some regularity [39] as follows. When several video objects are produced, users may interest in those video extremely. During this time, the frequency of request for the video is very high and the time slot of access to the video is very short. As time goes by, the interest for these video of user became weakened gradually or even forgotten. And then, the number of request for these video has decreased. Furthermore, it is found that the interest for emerging video of user attenuates or even forgets over time by analyzing the characteristics of video interest with changing. Most importantly, the feature of human forgetting is applied to the model of human behavior dynamics based on the change of interest, which simulates the characteristics attenuation of real users' interest in video over time in this paper. The formula of interest attenuation is proposed as follows.

$$Z(t, \kappa(j)) = ca^{-\frac{b}{a}}(t + \frac{1}{a})^{-\frac{b}{a}}e^{-\kappa(j)t}, \quad t \rightarrow \infty \quad (9)$$

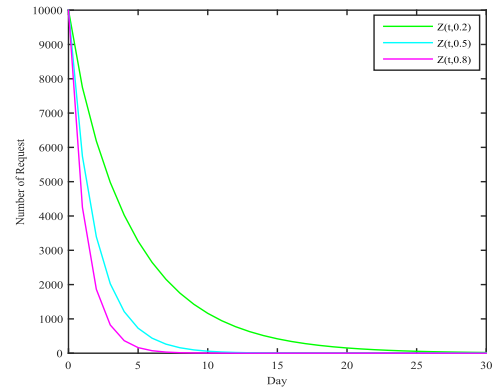


FIGURE 4. Interest attenuation over time.

Let  $Z(t, \kappa(j))$  denote the number changed of request for video object  $j$  as the elapse of time  $t$ . We formulate  $\kappa(j)$  as attenuation factor of video object  $j$ . The value of  $a, b$  and  $c$  are constant,  $a \neq 0$ . Besides,  $e$  indicates the natural base and  $O_j = Z(t_0, \kappa(j))$  represents the maximum requested number for video object  $j$  at time  $t = t_0$ .

The attenuation factor  $\kappa(j)$  indicates the attenuation characteristic of interest for video object  $\kappa(j)$ . Therefore, the attenuation characteristic is changed as the attenuation factor is different. As time goes on, the attenuation feature of request frequency for interest video from user has a mixed distribution form of power law and exponent when  $a > 0, b > 0, c > 0$  and attenuation factor  $\kappa(j) > 0$  in formula (9). To explicitly analyze the effect of attenuation factor on this formula, let  $a = 2, b = 0.1, c = 10000$ , then  $Z(t, \kappa(j)) = 10000 * 2^{-0.05}(t + 0.5)^{-0.05}e^{-\kappa(j)t}$ . The attenuation factor  $\kappa(j)$  is chosen as 0.2, 0.5 and 0.8 respectively to study the feature of decreased number for interest video objects requested. We observe that the requested number of interest video reduces faster since  $\kappa(j)$  becomes larger from Fig. 4. Hence, adjusting value of attenuation factor tracks the attenuation characteristics of request number for video object  $j$  to simulate the attenuation trend for interest video of users.

### C. THE PROCESS OF DYNAMIC DELIVERY

The interest for video objects of user shows attenuation or even forgets with time elapsing according to analyse the feature attenuation for interested video. In dynamic coupled video delivery process, the source server delivery video object to different surrogate servers based on interest attenuation and request for the video object. First of all, we generate  $N$  directed network graph file by time as seed. For each file, factors such as surrogate server, bandwidth and delay change over time. Next, the variable factor  $i$  is initialized. For each directed network graph file, the HMDT is executed. Finally, the effective delivery path and optimized cost are produced until all directed network graph files are included. The specific process of dynamic delivery for coupled video is shown in the Fig. 5.

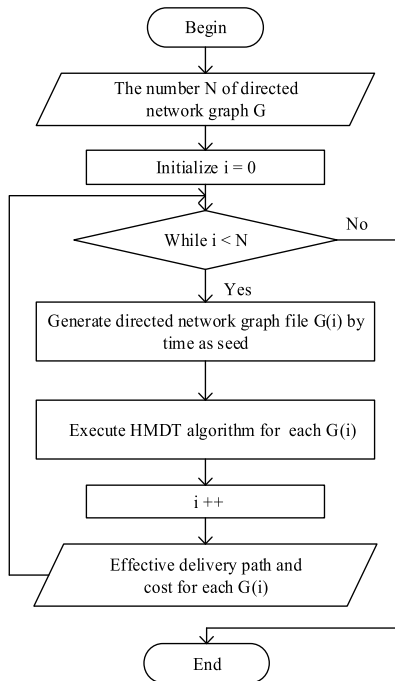


FIGURE 5. The process of dynamic delivery.

V. EXPERIMENTAL RESULTS

In this section, we evaluate the performance of HMDT algorithm in three aspects. Importantly, extensive simulations are performed to show that the improvement of our proposed algorithm compared with Fast Directed Steiner Tree (FDST) algorithm [40] and Approximate Steiner Tree Delivery (ASTD) algorithm [42] in various performance. FDST algorithm takes selected tree as the root node. Then, it searches a terminal that is closest to the selected tree and the selected tree extends a directed edge to the terminal. FDST algorithm repeats the extension steps until enough terminals are contained and outputs the selected tree. Furthermore, the ASTD algorithm selects the optimal path according to the density of the Steiner tree [42]. Given a tree and the cost of the tree  $c(T)$ , the density of the Steiner tree is defined as:  $\rho(T) = c(T)/k(T)$ , where  $k(T)$  represents the number of terminals in the tree  $T$ . To build this tree, the subtree with the minimal density is selected as the first level of the selection tree in ASTD algorithm. Next, the algorithm selects the minimal density subtree from remaining terminal nodes and add this subtree to the previous level of the selection tree. Finally, it repeat the selection until enough terminals are contained in the tree. In our simulation, the size of the video streaming is distributed with the normal distribution  $N(20k, 1GB)$ . The servers deployment obey the uniform distribution  $U(10, 100)$ , and surrogate servers are randomly selected among these servers.

A. IMPACT OF COEFFICIENT ON COST

We first evaluate the cost affected by the balance coefficient  $\alpha$  and  $\beta$  (see Fig. 6). In the simulation, we deploy 15 servers and select 10 surrogate servers among these servers.

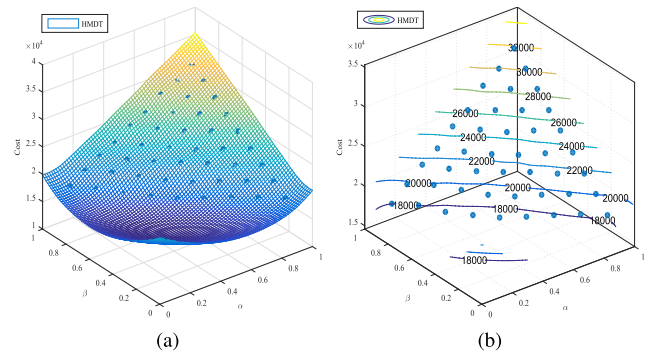


FIGURE 6. The impact of the coefficient  $\alpha$  and  $\beta$ . (a) Influenced of coefficient in three-dimensional surface map. (b) Influenced of coefficient in three-dimensional contour map.

The bandwidth was randomly selected from 800bps to 3000bps, and the delay was randomly allocated in the range of 1000ms to 2500ms in this experiment. Fig. 6 (a) and (b) show the influence of the balance coefficient on the cost from the three-dimensional surface map and the three-dimensional contour map respectively. As can be seen from Fig. 6 (a), when the sum of  $\alpha$  and  $\beta$  becomes larger, the cost of delivery rises. Especially, the yellow area of cost reaches the highest value. We can observe the effect of  $\alpha$  and  $\beta$  more intuitively in Fig. 6 (b). When the sum of  $\alpha$  and  $\beta$  remains unchanged, the delivery cost fluctuates within a smaller range. In addition, when the sum of  $\alpha$  and  $\beta$  remains 1, the cost is low. Particularly, when  $\alpha$  and  $\beta$  vary from 0.5 to 0.7, the consumed bandwidth and the produced delay can achieve a better balance which is acceptable for the users.

B. COST AFFECTED BY BANDWIDTH, DELAY AND OTHER FACTORS

Next, we analyze factors that influence the delivery cost as bandwidth increased, such as balance coefficient, the number of surrogate server and the directed edges (see Fig. 7). In this simulation, the delay is randomly allocated in the range of 1000ms to 2500ms, and the specific parameter settings are given for each figure (see Table 1). It can be seen from the comparison between Fig. 7 (a) and (b) that the cost of Fig. 7 (b) increase slowly as the bandwidth becoming larger. We can note that the balanced cost of  $\alpha = 0.5, \beta = 0.5$  is better than that of  $\alpha = 0.2, \beta = 0.8$ . This result shows that the balanced delivery cost is optimal when the sum of coefficient is 1 and the difference between  $\alpha$  and  $\beta$  is small. Additionally, we explore how the number of surrogate servers affect the delivery cost when different number of surrogate servers is deployed in Fig. 7 (b) and (c). Experimental analysis shows that the increased number of surrogate servers leads to larger cost when the number of servers is fixed. Then, we change the number of directed edges to explore whether the number of edges has an impact on the delivery cost. By comparing Fig. 7 (b) and(d), we can see that the delivery cost is relatively lower with more edges. The analysis results of the above experimental results show that parameter setting of different have a greater impact on delivery cost. Importantly, our

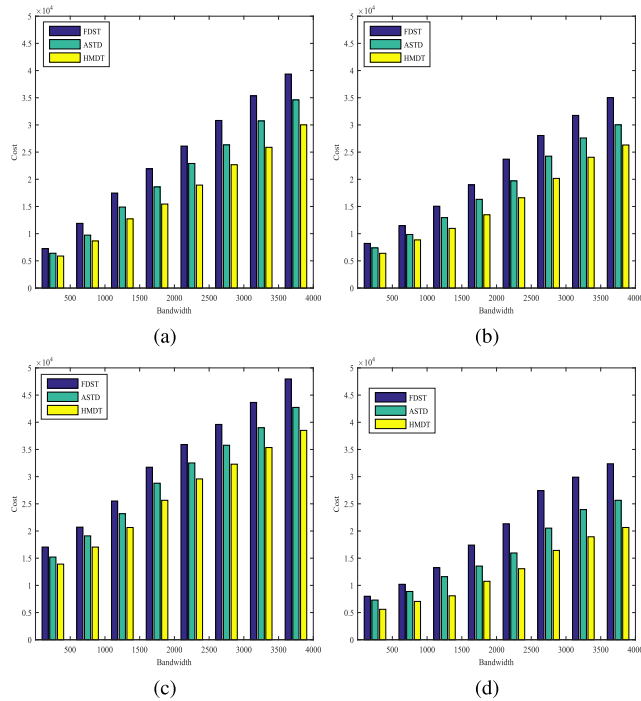


FIGURE 7. Influence on the bandwidth cost.

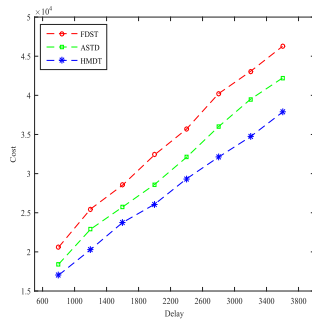


FIGURE 8. Cost vs. delay.

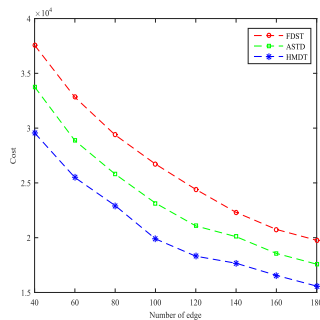


FIGURE 9. Cost vs. number of directed edges.

proposed HMDT algorithm exhibits effective performance and achieves lower cost than FDST and ASTD algorithm.

In Fig. 8, we explore the delay effect on cost. We set  $\alpha = 0.5$ ,  $\beta = 0.5$  and deploy 20 servers, randomly selected 10 surrogate servers, 40 directed edges. The bandwidth ranges between 800bps and 3000bps. It can be seen from the graph

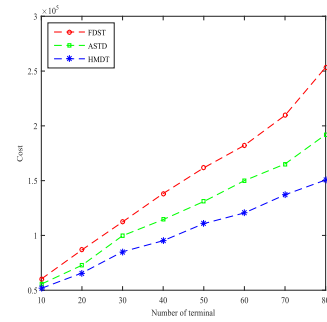


FIGURE 10. Cost vs. number of terminals.

that the delivery cost keeps rising as the delay increases. In other words, the longer delay leads to higher cost. Moreover, our proposed HMDT algorithm achieves lower delivery cost than FDST and ASTD algorithm.

In Fig. 9, we study the influence of the number of directed edges. We set  $\alpha = 0.5$ ,  $\beta = 0.5$  and deploy 20 servers and 15 surrogate servers in the scenario. The bandwidth was randomly selected from 800bps to 3000bps, and the delay was randomly allocated in the range of 1000ms to 2500ms in this experiment. As we can see from Fig. 9, the delivery cost is declining as the number of edges increases. Consequently, the delivery cost of the HMDT algorithm is lower than FDST and ASTD algorithm.

Fig. 10 and Fig. 11 show the effect on delivery cost of the number of surrogate server and the number of serve respectively. In this simulation, we set  $\alpha = 0.5$ ,  $\beta = 0.5$ , and randomly deploy 200 directed edges. The delay was randomly allocated in the range of 1000ms to 2500ms, and the bandwidth was randomly distributed from 800bps to 3000bps in this experiment. As for the influence of the number of surrogate servers, we randomly deploy 100 servers and select surrogate servers based on demands of users among servers. Fig. 10 shows that the delivery cost is rising when the number of surrogate servers increases. In regard to the influence of the number of servers in Fig. 11, we randomly deploy 15 surrogate servers and keep the number of surrogate servers unchanged. As demonstrated in this figure, the delivery cost grows rapidly as the number of servers increases. During the simulation, we can find that the increasing of the number of surrogate servers or the number of servers will result in higher delivery cost, and our proposed HMDT algorithm is superior to FDST and ASTD algorithm in performance.

C. INFLUENCE OF PERSONALIZED DEMANDS ON COST

Finally, we conduct different methods for video delivery and analyze these methods effected on cost. In this simulation, the bandwidth ranges between 800bps and 3000bps and the delay is randomly allocated from 1000ms to 2500ms. We set  $\alpha = 0.5$ ,  $\beta = 0.5$ , and randomly deploy 90 directed edges. The algorithms of Passive, Proactive, BDDT(Bandwidth-Delay Delivery Tree) and HMDT are conducted to explore the different strategies influenced on cost (see Fig. 12). However, DTLM algorithm not taken the factor of personalized



TABLE 1. Parameter settings.

Experimental figure	$\alpha, \beta$	Number of server	Number of surrogate server	Number of edge
(a)	$\alpha = 0.2, \beta = 0.8$	20	10	40
(b)	$\alpha = 0.5, \beta = 0.5$	20	10	40
(c)	$\alpha = 0.5, \beta = 0.5$	20	15	40
(d)	$\alpha = 0.5, \beta = 0.5$	20	10	60

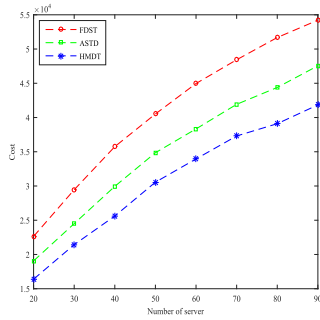


FIGURE 11. Cost vs. number of servers.

demands into account for delivery cost. It can be seen from the experimental analysis that HMDT algorithm provide the lowest cost. Additionally, the delivery cost of Passive algorithm is lower than Proactive algorithm with a few of servers. However, as the number of server increase, the delivery cost of Passive algorithm exceed the Proactive algorithm extremely. Importantly, we note that HMDT algorithm provide the lowest cost with considering personalized demands.

We explore interest attenuation effect on delivery cost since the interest for video objects of people vary over time. In this simulation, 100 video objects with similar attenuation distribution are delivered in a period of time. Let  $\kappa(j) = 0.2$ ,  $\kappa(j) = 0.5$ ,  $\kappa(j) = 0.8$  respectively,  $Z(t_0, \kappa(j)) = 10000$ . We deploy 30 servers and 10 surrogate servers, 50 directed edges. The bandwidth was randomly allocated between 800bps and 3000bps. As we can see from Table 2, the higher interest degree of users with a great deal of requested number for video, it provides lower cost. Conversely, the exorbitant delivery cost is produced as attenuation interest of user with little requested number for the video. Consequently, the delivery cost increases as attenuation interest of user over time.

Here, we analyze how values of interest affect the performance of delivery cost. We deploy 40 servers, randomly selected 15 surrogate servers, 100 directed edges and choose several video objects with the maximum requested number 10000 from origin server in the scenario. We divide the maximum requested number into 1000 and calculate interest value  $\theta$  according to the request number for these video objects from surrogate servers to the origin server. Fig. 13 shows that  $\frac{1}{\theta}$  is inversely proportional to delivery cost. In other words, the larger delivery cost is obtained as the lower degree of interest for video objects with smaller  $\frac{1}{\theta}$ . Otherwise, the higher degree of interest for video objects with bigger  $\frac{1}{\theta}$  achieves lower delivery cost steadily. Accordingly, we infer

TABLE 2. Interest attenuation effect on cost.

Parameters	Number of request	Cost
$\kappa(j) = 0.2$	10000	50815
	8000	62327
	6000	70012
	4000	111054
	2000	169687
$\kappa(j) = 0.5$	10000	51138
	8000	64305
	6000	69876
	2000	190529
$\kappa(j) = 0.8$	10000	51276
	8000	63531
	6000	71103
	2000	183256

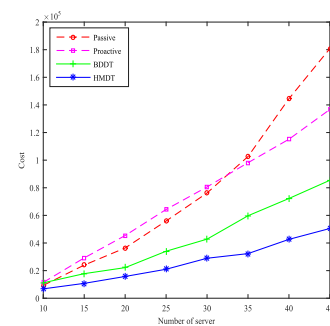


FIGURE 12. Different methods for deliver video.

that the larger  $\theta$  which indicated lack of interest for video objects brings larger delivery cost. Conversely, the smaller the  $\theta$  represents the higher degree interest of user for video objects and HMDT algorithm achieves lower delivery cost.

In dynamic networks, we explore the influence of different interest values on delivery cost at varying time. In this simulation, we assume that the size of video objects which is delivered from the origin server is equal in different time. We deploy 40 servers, randomly selected 15 surrogate servers, 100 directed edges and the maximum requested

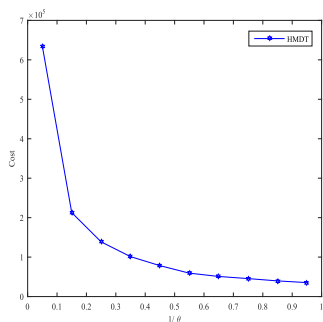


FIGURE 13. Cost vs. interest value.

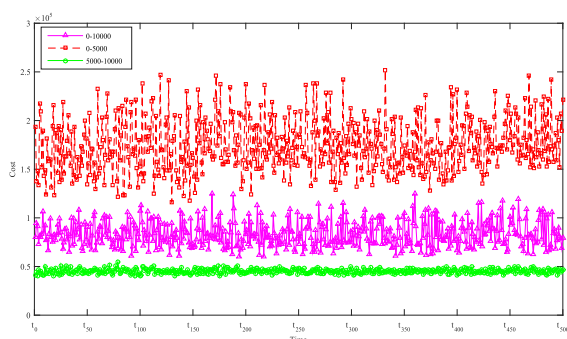


FIGURE 14. Cost vs. range of interest value at different time slots.

number for video objects is 10000. On one hand, we study unequal interest value  $\theta$  influence of delivery when the number of requests for video streaming varies within a certain range at different time. On the other hand, requested number of video objects are compared in different ranges to explore how the size of interest value  $\theta$  effected on cost. Fig. 14 shows that the HMDT algorithm has a larger cost when request number of video objects in the range of 0 to 5000 and the delivery cost is lower with the request number of video objects from 5000 to 10000 at different time. Accordingly, when the request number varies from 0 to 10000, the delivery cost fluctuates obviously. As the request number between 0 and 5000, the delivery cost is highest and unstable. Importantly, when the requested number for video objects varies from 5000 to 10000, the cost is lower obviously and stable. Therefore, we infer that the delivery cost is lower and the variation is stable relatively as  $\frac{1}{2} < \frac{1}{\theta} \leq 1$  in the process of coupled video delivery at different time slots.

## VI. CONCLUSION AND FUTURE WORK

In this paper, we propose a CO-CVDM (Cost Optimization for Coupled Video Delivery Model) which combines coupled proactive video delivery and coupled reactive video delivery. The factors of bandwidth consumption, delay performance and personalized demand are into account jointly to optimize delivery cost. In this model, we formulate the coupled video delivery process as a cost minimization problem and construct a multicast distribution tree for the video delivery. Since the problem is NP-hard, the heuristic multicast delivery tree (HMDT) algorithm is proposed to provide an

optimal approximately cost. Additionally, we explore the feature of interest attenuation over time and apply it to the field of dynamic video delivery networks. The process of video delivery is truncated into a sequence of static graphs and the dynamic delivery for personalized demand model is constructed to meet dynamic requirement for live video of user.

In addition, the substance of cost optimization for the coupled video delivery designed in this paper is theoretical analysis and it lacks application in nature mobile networks. In future, we plan to apply the contribution to reality mechanism of video delivery in mobile wireless networks in order to reduce delivery cost for online video.

## REFERENCES

- [1] J. Chen, Z. Chen, D. Lu, C. Lyu, G. Zhang, X. Zheng, and H. Liu, "Cost-effective coupled video distribution network," in *Proc. Conf. Comput. Supported Cooperat. Work Social Comput.*, 2019, pp. 115–128.
- [2] "Cisco visual networking index: Forecast and methodology, 2016–2021," Cisco Systems, San Jose, CA, USA, White Paper 1513879861264127, 2017.
- [3] Y. Liu, D. Lu, G. Zhang, J. Tian, and W. Xu, "Q-learning based content placement method for dynamic cloud content delivery networks," *IEEE Access*, vol. 7, pp. 66384–66394, 2019.
- [4] "Cisco visual networking index: Forecast and methodology, 2014–2019," Cisco Systems, San Jose, CA, USA, White Paper, 2015.
- [5] J. Liu, N. Kato, J. Ma, and N. Kadowaki, "Device-to-device communication in LTE-advanced networks: A survey," *IEEE Commun. Surveys Tuts.*, vol. 17, no. 4, pp. 1923–1940, 4th Quart., 2017.
- [6] F. Dobrian, V. Sekar, A. Awan, I. Stoica, D. Joseph, A. Ganjam, J. Zhan, and H. Zhang, "Understanding the impact of video quality on user engagement," *Commun. ACM*, vol. 56, no. 3, pp. 91–99, Mar. 2013.
- [7] F. Wang, J. Liu, M. Chen, and H. Wang, "Migration towards cloud-assisted live media streaming," *IEEE/ACM Trans. Netw.*, vol. 24, no. 1, pp. 272–282, Feb. 2016.
- [8] K. Katsalis, V. Sourlas, T. Korakis, L. Tassioulas, "A cloud-based content replication framework over multi-domain environments," in *Proc. IEEE Int. Conf. Commun.*, Jun. 2014, pp. 2926–2931.
- [9] M. Salahuddin, H. Elbiaze, W. Ajib, and R. Glitho, "Social network analysis inspired content placement with QoS in cloud based content delivery networks," in *Proc. IEEE Global Commun. Conf.*, Dec. 2015, pp. 1–6.
- [10] N. Carlsson, D. Eager, A. Gopinathan, and Z. Li, "Caching and optimized request routing in cloud-based content delivery systems," *Perform. Eval.*, vol. 79, no. 4, pp. 38–55, Sep. 2014.
- [11] C. Papagianni, A. Leivadreas, and S. Papavassiliou, "A cloud-oriented content delivery network paradigm: Modeling and assessment," *IEEE Trans. Dependable Secure Comput.*, vol. 10, no. 5, pp. 287–300, Sep./Oct. 2013.
- [12] M. Garetto, E. Leonardi, and S. Traverso, "Efficient analysis of caching strategies under dynamic content popularity," in *Proc. Comput. Commun.*, 2015, pp. 2263–2271.
- [13] E. Bastug, M. Bennis, and M. Debbah, "Cache-enabled small cell networks: Modeling and tradeoffs," in *Proc. Int. Symp. Wireless Commun. Syst.*, 2014, pp. 649–653.
- [14] X. Liu, Y. Liu, N. N. Xiong, N. Zhang, A. Liu, H. Shen, and C. Huang, "Construction of large-scale low-cost delivery infrastructure using vehicular networks," *IEEE Access*, vol. 6, no. 1, pp. 21482–21497, 2018.
- [15] O. V. Aram, S. Yousefi, and M. Solimanpur, "Joint server selection and replica placement in urban content delivery networks," *Int. J. Oper. Res.*, vol. 25, no. 3, pp. 288–306, 2016.
- [16] J. Wu, B. Cheng, M. Wang, and J. Chen, "Energy-efficient bandwidth aggregation for delay-constrained video over heterogeneous wireless networks," *IEEE J. Sel. Areas Commun.*, vol. 25, no. 11, pp. 30–49, Jan. 2017.
- [17] D. Lu, X. Huang, G. Zhang, X. Zheng, and H. Liu, "Trusted device-to-device based heterogeneous cellular networks: A new framework for connectivity optimization," *IEEE Trans. Veh. Technol.*, vol. 67, no. 11, pp. 11219–11233, Nov. 2018.
- [18] H. Gong, L. Fu, X. Fu, L. Zhao, K. Wang, and X. Wang, "Distributed multicast tree construction in wireless sensor networks," *IEEE Trans. Inf. Theory*, vol. 63, no. 1, pp. 280–296, Jan. 2017.

- [19] X. Fu, Z. Xu, Q. Peng, J. You, L. Fu, X. Wang, and S. Lu, "ConMap: A novel framework for optimizing multicast energy in delay-constrained mobile wireless networks," in *Proc. ACM Int. Symp.*, 2017, pp. 1–10.
- [20] Y. Jin, Y. Wen, K. Guan, D. Kilper, and H. Xie, "Toward monetary cost effective content placement in cloud centric media network," in *Proc. IEEE Int. Conf. Multimedia Expo.*, Jul. 2013, pp. 1–6.
- [21] R. Han, Y. Gao, C. Wu, and D. Lu, "An effective multi-objective optimization algorithm for spectrum allocations in the cognitive-radio-based Internet of Things," *IEEE Access*, vol. 6, pp. 12858–12867, 2018.
- [22] J. Yun, M. Piran, and D. Suh, "QoE-driven resource allocation for live video streaming over D2D-underlaid 5G cellular networks," *IEEE Access*, vol. 6, pp. 72563–72580, 2018.
- [23] L. Zeng, S. Xu, Y. Wang, K. B. Kent, D. Bremner, and C. Xu, "Toward cost-effective replica placements in cloud storage systems with QoS-awareness," *Softw., Pract. Exp.*, vol. 47, no. 6, pp. 813–829, 2017.
- [24] J. Wu, C. Yuen, B. Cheng, Y. Yang, M. Wang, and J. Chen, "Bandwidth-efficient multipath transport protocol for quality-guaranteed real-time video over heterogeneous wireless networks," *IEEE Trans. Commun.*, vol. 64, no. 6, pp. 2477–2493, Jun. 2016.
- [25] Y. Zhou, L. Chen, C. Yang, and D. M. Chiu, "Video popularity dynamics and its implication for replication," *IEEE Trans. Multimedia*, vol. 17, no. 8, pp. 1273–1285, Aug. 2015.
- [26] A. Brodersen, S. Scellato, and M. Wattenhofer, "YouTube around the world: Geographic popularity of videos," in *Proc. Int. Conf. World Wide Web*, 2012, pp. 241–250.
- [27] S. Li, J. Xu, M. van der Schaar, and W. Li, "Popularity-driven content caching," in *Proc. IEEE Int. Conf. Comput. Commun.*, Apr. 2016, pp. 1–9.
- [28] B. Blaszczyzyn and A. Giovanidis, "Optimal geographic caching in cellular networks," in *Proc. IEEE Int. Conf. Commun.*, Jun. 2015, pp. 3358–3363.
- [29] G. Zhang, D. Lu, and H. Liu, "Strategies to utilize the positive emotional contagion optimally in crowd evacuation," *IEEE Trans. Affect. Comput.*, to be published. doi: 10.1109/TAFFC.2018.2836462.
- [30] D. Lu, X. Huang, W. Zhang, and J. Fan, "Interference-aware spectrum handover for cognitive radio networks," *Wireless Commun. Mobile Comput.*, vol. 14, no. 11, pp. 1099–1112, 2014.
- [31] J. Tadrous, A. Eryilmaz, and H. El Gamal, "Proactive content download and user demand shaping for data networks," *IEEE/ACM Trans. Netw.*, vol. 23, no. 6, pp. 1917–1930, Dec. 2015.
- [32] G. Quer, I. Pappalardo, B. D. Rao, and M. Zorzi, "Proactive caching strategies in heterogeneous networks with device-to-device communications," *IEEE Trans. Wireless Commun.*, vol. 17, no. 8, pp. 5270–5281, Aug. 2018.
- [33] K. Wang, Z. Chen, and H. Liu, "Push-based wireless converged networks for massive multimedia content delivery," *IEEE Trans. Wireless Commun.*, vol. 13, no. 5, pp. 2894–2905, May 2014.
- [34] S. Borst, V. Gupta, and A. Walid, "Distributed caching algorithms for content distribution networks," in *Proc. Conf. Inf. Commun.*, 2010, pp. 1–9.
- [35] X. Guan and B. Choi, "Push or pull?: Toward optimal content delivery," in *Proc. IEEE Int. Conf. Commun.*, Jun. 2014, pp. 1–5.
- [36] D. Lu, B. Hu, X. Zheng, H. Liu, and G. Zhang, "Session-based cloud video delivery networks in mobile Internet," *J. Internet Technol.*, vol. 18, no. 7, pp. 1561–1571, 2017.
- [37] Q. Jia, R. Xie, T. Huang, J. Liu, and Y. Liu, "The collaboration for content delivery and network infrastructures: A survey," *IEEE Access*, vol. 5, pp. 18088–18106, 2017.
- [38] H. Guo, S. Marston, and Y. Chen, "Push or pull? Design of content delivery systems," *Decis. Sci.*, vol. 46, no. 5, pp. 937–960, 2015.
- [39] R. Devooght and H. Bersini, "Long and short-term recommendations with recurrent neural networks," in *Proc. Conf. User Modeling ACM*, 2017, pp. 13–21.
- [40] M. Hsieh, H. Wu, and M. Tsai, "FasterDSP: A faster approximation algorithm for directed Steiner tree problem," *J. Inf. Sci. Eng.*, vol. 22, no. 6, pp. 1409–1425, 2006.
- [41] Y. Chen and C. Shen, "Performance analysis of smartphone-sensor behavior for human activity recognition," *IEEE Access*, vol. 5, pp. 3095–3110, 2017.
- [42] M. Charikar, C. Chekuri, T.-Y. Cheung, Z. Dai, A. Goel, S. Guha, and M. Li, "Approximation algorithms for directed Steiner problems," *J. Algorithms*, vol. 33, no. 1, pp. 73–91, 1999.



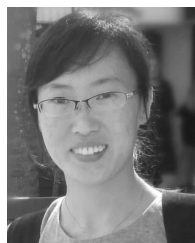
**JING CHEN** is currently pursuing the M.S. degree with the School of Information Science and Engineering, Shandong Normal University, Jinan, China. Her research interests include video delivery networks and cloud computing.



**DIANJI LU** received the Ph.D. degree in computer science from the Institute of Computing Technology, Chinese Academy of Science, Beijing, China, in 2012. He is currently an Associate Professor with the School of Information Science and Engineering, Shandong Normal University, Jinan, China. His research interests include the cognitive Internet of Things, heterogeneous cellular networks, and cloud computing.



**GUIJUAN ZHANG** received the Ph.D. degree in computer science from the Institute of Computing Technology, Chinese Academy of Science, Beijing, China, in 2011. She is currently an Associate Professor with the School of Information Science and Engineering, Shandong Normal University, Jinan, China. Her research interests include distributed computing and computational intelligence.



**JINGPING QIAO** received the Ph.D. degree from Shandong University, China, in 2018. She is currently a Lecturer with the School of Information Science and Engineering, Shandong Normal University, China. Her research interests include physical layer security, cooperative (relay) communications, signal processing for communications, and simultaneous wireless information and power transfer.



**PINGSHAN LIU** received the Ph.D. degree in computer science from the Institute of Computing Technology, Chinese Academy of Science, Beijing, China, in 2014. He is currently an Associate Professor with the Business School, Guilin University of Electronic Technology, Guilin, China. His research interests include content delivery networks, streaming media communication networks, and cloud computing.



**REN HAN** received the Ph.D. degree in computer science from the University of Chinese Academy of Sciences, Beijing, China, in 2014. He is currently a Lecturer with the School of Optical-Electrical and Computer Engineering, University of Shanghai for Science and Technology, China. His research interests include cognitive radio networks, wireless sensor networks, and the Internet of Things.

...